

# Multifractal Analysis and Its Application in Marine Data Analysis

Xi Lei <sup>1</sup>, Liping Wang <sup>1,\*</sup>, Yi Kou <sup>2</sup>, Fang Wu <sup>3</sup>, Shaoxun Liu <sup>4</sup>, and Chunlei Wang <sup>5</sup>

<sup>1</sup>School of Mathematical Sciences, Ocean University of China, Qingdao, China; weiborulan@126.com

<sup>2</sup>Molecular and Computational Biology, University of Southern California, Los Angeles, USA; yikou@usc.edu

<sup>3</sup>Statistics and Applied Probability, University of California Santa Barbara, Santa Barbara, USA; fangwu0703@gmail.com

<sup>4</sup>Dornsife College, University of Southern California, Los Angeles, USA; shaoxunl@usc.edu

<sup>5</sup>School of Computer & Communication Engineering, University of Science & Technology Beijing, China; wangcl\_ustb@qq.com

\* Correspondence: wlpjsh@163.com

**Abstract:** By taking the over-threshold extremum data of Wusong Station in Shanghai as a sample, through the calculation of Hurst index, correlation dimension and fractal dimension, this study reveals that there are obvious fractal patterns in the tidal levels from disaster causing factors such as storm water increase and upstream flood. The combined return level is derived based on the fractal theory for the storm water increase and the upstream flood. The return levels for the storm water increase and upstream flood are 0.9012 meters and 0.3126 meters respectively when the return period is 20 years; 1.0785 meters and 0.4093 meters when the return period is 50 years; and 1.2494 meters and 0.5277 when the return period is 100 years.

**Keywords:** self-similarity; fractal; return level; typhoon storm surge

## 1. Introduction

In recent years, storm surges have occurred frequently with increasing destructive power, which has greatly affected the development of coastal cities, resulting in huge economic losses. To protect the coast and estuary areas from the big, high tides and the storm surges, the seawall is built to resist strong wind and waves, which also plays an important role in various other coastal protection projects. The biggest factor affecting and destroying the seawalls comes from the occurrence of extreme sea conditions. In recent years, typhoons have frequently visited the coastal areas of China, and they are often accompanied by strong winds, heavy rains and storm surges. If the storm surge coincides with the big astronomical tide, it will often cause the water level in the affected area to soar. Once it meets the runoff water increase caused by the upstream flood peak from the rainstorm, the resulted high water level will be easily flowing over the seawall top, imposing a great flooding risk. For example, the 11th typhoon landed in Wenling, Zhejiang Province in 1997, and coincided with the high water level from the astronomical tide. The seawall built failed to resist such extreme conditions, and thus resulted in breaches with subsequent sea water intrusion and flash

floods for more than 3 days, which had a direct economic loss to be more than 4.5 billion yuan [2].

The effects of storm surges and tropical cyclones can lead to fast water increase and add more uncertainties to the upstream flood, which is the root cause of unexpected storm surge disaster. Therefore, to mitigate and prevent the potential loss, it is of great significance to accurately calculate the storm water and upstream floods parameters, carry out risk analysis, forecast and give early warnings for such disasters.

When studying the laws of hydrological movement, the influence of time scales on hydrological phenomena cannot be ignored. For situations in the short-term or a foreseeable period, the deterministic methods are generally adopted [1-4]. These research methods are all carried out spatially from a relatively macro perspective. As the scale increases, the complexity and uncertainty also accumulate accordingly, and the deterministic method is no longer applicable [5-10]. At present, in the risk analysis of seawall overflow flooding, the analysis of the natural characteristics of the load for the seawall from the time scale is missing.

There are widespread phenomena of disorder, chaos and irregularity in hydrology and water resources. A large number of studies have shown that there are some laws behind these complex phenomena: that is, there are some forms of similarity between the parts and the whole under statistical calculation, which is also known as statistical self-similarity. Fractal theory is a science that describes many irregular, disordered phenomena and irregularities in nature. It uses non-integer dimensions to quantitatively describe the complexity of objective things and has been rapidly developing in many disciplines. Because of the simple laws often existing behind the complex situations, fractal theory uses self-similarity to gain insight into the hidden regular structure in the chaotic phenomena. Fortunately, self-similarity phenomena are ubiquitous in hydrological systems [11-14]. For example, a watershed with a dendritic branch is a system with typical self-similarity: a sub-basin in a dendritic bifurcation can be enlarged to the scale of the entire basin with very good similarity [15]; the coastline also has self-similarity: by amplifying a portion of the coastline, it looks similar to

the original entire coastline [16-17]; when floods are seen as a response of the hydrological system to precipitation inputs, the distribution also has self-similarity in both time and space. Because hydrological phenomena generally possess self-similar features, the fractal theory created by Mandelbrot can thus reveal the fine structure of complex hydrological phenomena on the time scale, which has drawn great attentions nowadays [18-21].

This paper chose to study the 20-year storm water increase and upstream flood data of Datong Hydrological Station in Wusongkou, Shanghai. By means of applying self-similarity principle, considering the combination of tidal level, storm water increase and upstream flood, it reveals the natural characteristics and the mutual restraint relationships of the storm water increase and upstream flood on time scale. Additionally, based on the fractal theory, the combined return level of the storm water increase and the upstream floods are derived. The results obtained are proposed for marine engineering design to prevent and reduce flood disaster in Shanghai area.

**2. Distribution Pattern of Marine Environmental Factors Based on Fractal Theory**

Fractal distribution is sometimes called Pareto distribution, Pareto-Levy distribution or Stable-Paretian distribution [22]. Statistical self-similarity, which is also known as scale invariance, is often described as a situation in which the statistical characteristics remain the same under different time increments, or that the distribution remains as the same shape despite the adjusted time scale. The characteristic function for the fractal distribution can be expressed as follows:

$$\Phi_X(t) = E[\exp(itX)] = \begin{cases} \exp\left\{-\gamma^\alpha |t|^\alpha \cdot [1 - i\beta \frac{t}{|t|} \cdot \tan \frac{\pi\alpha}{2}] + i\delta t\right\}, \alpha \neq 1; \\ \exp\left\{-\gamma^\alpha |t|^\alpha \cdot [1 + i\beta \frac{2}{\pi} \cdot \ln |t|] + i\delta t\right\}, \alpha = 1. \end{cases} \quad (1)$$

Its logarithmic form can be expressed as:

$$\ln \Phi_X(t) = \ln(f(t)) = \begin{cases} i\delta t - \gamma^\alpha |t|^\alpha \cdot [1 - i\beta \frac{t}{|t|} \cdot \tan \frac{\pi\alpha}{2}], \alpha \neq 1; \\ i\delta t - \gamma^\alpha |t|^\alpha \cdot [1 + i\beta \frac{2}{\pi} \cdot \ln |t|], \alpha = 1. \end{cases} \quad (2)$$

In which  $\alpha, \beta, \delta, \gamma$  are the parameters.  $\alpha$  is the fractal dimension of the time series probability space, and it is also the characteristic index, which indicates the characteristics of the distribution, and measures the kurtosis and the tailing of the distribution at  $\delta$ .  $\alpha \in (0, 2]$ , its value affects the nature of the time series. The smaller the value, the more observations farther away from the center and the thicker for the tail.  $\beta$  is the skewness index, measuring the skewness.  $\beta \in [-1, 1]$ , which determines the degree of symmetry for the distribution. It is symmetrical when  $\beta = 0$ . And the greater the degree of skewness, the larger the absolute value when  $|\beta| \neq 0$ .  $\delta$  is the positional parameter of the mean,  $\delta \in (-\infty, +\infty)$ , which indicates the symmetrical

position of the distribution.  $\gamma$  is the adjustable scale parameter,  $\gamma \in (0, +\infty)$ , it controls the width of the distribution curve: the larger the value, the wider the distribution curve would be.

Let  $F_X$  be the cumulative distribution function of the fractal distribution, the relationship between the characteristic functions of the fractal distribution and the characteristic function of the fractal distribution can be derived by the Riemann-Stichels integral:

$$\Phi_X(t) = E[\exp(itX)] = \int_{-\infty}^{+\infty} e^{itx} dF_X(x) \quad (3)$$

If  $f_X$  is a probability density function of a fractal distribution, its relationship with the characteristic function of the fractal distribution is:

$$\Phi_X(t) = E[\exp(itX)] = \int_{-\infty}^{+\infty} e^{itx} f_X(x) dx \quad (4)$$

With the characteristic function, we can find the moment by deriving the derivative of the characteristic function.

Theorem. Let the random variable  $X$  obey the fractal distribution  $X$ . If the characteristic function  $\Phi_X(t)$  of the random variable  $X$  is absolutely integrable on  $R_1$ , then  $X$  is a continuous random variable with a density

function  $f_X$ , and  $X_1 = x$ ,  

$$f_X(x) = \frac{1}{2\pi} \int_{-\infty}^{+\infty} e^{-itx} \Phi_X(t) dt \quad (5)$$

Proof:

By

$$\tilde{F}_X(x) = \frac{F_X(x+0) + F_X(x)}{2}$$

and

$$\frac{F_X(x_2+0) + F_X(x_2)}{2} - \frac{F_X(x_1+0) + F_X(x_1)}{2},$$

$$= \lim_{\tau \rightarrow +\infty} \frac{1}{2\pi} \int_{-\tau}^{+\tau} \frac{e^{-itx_1} - e^{-itx_2}}{it} \Phi_X(t) dt$$

Let  $x_2 = x + \Delta x$  (here  $\Delta x > 0$ ),  $x_1 = x$ , then we have:

$$\begin{aligned} & \tilde{F}_X(x + \Delta x) - \tilde{F}_X(x) \\ &= \frac{1}{2\pi} \lim_{\tau \rightarrow +\infty} \int_{-\tau}^{+\tau} \frac{e^{-itx} - e^{-it(x+\Delta x)}}{it} \Phi_X(t) dt \\ &= \frac{1}{2\pi} \lim_{\tau \rightarrow +\infty} \int_{-\tau}^{+\tau} \frac{1 - e^{-it\Delta x}}{it} e^{-itx} \Phi_X(t) dt \\ &= \frac{1}{\pi} \lim_{\tau \rightarrow +\infty} \int_{-\tau}^{+\tau} \frac{\sin t \frac{\Delta x}{2}}{t} \cdot e^{-it(x+\frac{\Delta x}{2})} \Phi_X(t) dt \end{aligned}$$

Thus there is:

$$\begin{aligned} & \frac{\tilde{F}_X(x + \Delta x) - \tilde{F}_X(x)}{\Delta x} \\ &= \frac{1}{2\pi} \lim_{\tau \rightarrow +\infty} \int_{-\tau}^{+\tau} \frac{\sin t \frac{\Delta x}{2}}{t \Delta x} \cdot e^{-it(x+\frac{\Delta x}{2})} \Phi_X(t) dt \end{aligned} \quad (6)$$

Since

$$\left| \frac{\sin t \frac{\Delta x}{2}}{\frac{t \Delta x}{2}} \cdot e^{-it(x+\frac{\Delta x}{2})} \Phi_X(t) \right| \leq |\Phi_X(t)|$$

And  $\Phi_X(t)$  is absolute integrable, so the right end of (6) is uniformly converged. And because of any finite interval of  $t$ , the right end of (6) is uniformly converged to  $e^{-itx} \Phi_X(t)$  by the integral function, so there is:

$$\begin{aligned} & \lim_{\Delta x \rightarrow 0} \frac{\tilde{F}_X(x+\Delta x) - \tilde{F}_X(x)}{\Delta x} \\ &= \lim_{\Delta x \rightarrow 0} \frac{1}{2\pi} \int_{-\infty}^{+\infty} \frac{\sin t \frac{\Delta x}{2}}{\frac{t \Delta x}{2}} \cdot e^{-it(x+\frac{\Delta x}{2})} \Phi_X(t) dt \\ &= \frac{1}{2\pi} \int_{-\infty}^{+\infty} \lim_{\Delta x \rightarrow 0} \frac{\sin t \frac{\Delta x}{2}}{\frac{t \Delta x}{2}} \cdot e^{-it(x+\frac{\Delta x}{2})} \Phi_X(t) dt \\ &= \frac{1}{2\pi} \int_{-\infty}^{+\infty} e^{-itx} \Phi_X(t) dt \end{aligned} \tag{7}$$

For  $\Delta x < 0$ , we can also get (7) similarly.

It is seen from equation (7) that the derivative of  $\tilde{F}_X(x)$  exists and thus  $\tilde{F}_X(x)$  is continuous, so there is  $\tilde{F}_X(x) = F_X(x)$ , and

$$\tilde{F}_X'(x) = F_X'(x) = \frac{1}{2\pi} \int_{-\infty}^{+\infty} e^{-itx} \Phi_X(t) dt .$$

Furthermore, the above method can be used to prove that  $F_X'(x)$  is continuous, bounded and non-negative, thus there is:

$$F_X(x) = \int_{-\infty}^x F_X'(x) dx$$

Therefore  $X$  is a continuous type and its density function is

$$f_X(x) = F_X'(x) = \frac{1}{2\pi} \int_{-\infty}^{+\infty} e^{-itx} \Phi_X(t) dt .$$

End of proof.

In engineering applications, Equation (5) can be obtained as follows: Let the random variable  $X$  obey the fractal distribution  $X \sim S_\alpha(\gamma, \beta, \delta)$ , then there is:

$$\begin{aligned} \int_R |\Phi(t)| dt &= \int_R e^{-\gamma|t|^\alpha} dt = 2 \int_0^\alpha e^{-\gamma|t|^\alpha} dt \\ &= 2 \int_0^1 e^{-\gamma|t|^\alpha} dt + 2 \int_1^\alpha e^{-\gamma|t|^\alpha} dt \end{aligned} \tag{8}$$

Since  $\gamma > 0$ , and under normal circumstances,  $\alpha < 1$ , so there is:

$$0 < 2 \int_0^1 dt + 2 \int_1^\alpha e^{-\gamma t} dt < 2 + 4\gamma < \infty \tag{9}$$

Since the characteristic function is absolute integrable, so its density function is:

$$f(x) = \frac{1}{2\pi} \int_{-\infty}^{+\infty} e^{-itx} \Phi(t) dt = \int_{-\infty}^{+\infty} e^{i2\pi\omega x} \Phi(2\pi\omega) d\omega \tag{10}$$

From the fast Fourier transformation of  $\Phi(t)$ , we can have

$$\Phi(t) = \sum_{k=0}^N \left[ \frac{1}{N} \sum_{n=0}^{N-1} \Phi\left(\frac{2n\pi}{N}\right) e^{ik\frac{2n\pi}{N}} \right] e^{ikt} \tag{11}$$

For  $N = 2^m$ ,  $m = N$ , divide the entire integration range into  $N+1$  points with an interval of  $s$ . For each

point, there is  $\omega_k = (k-1 - \frac{N}{2})s, k = 1, 2, \dots, N+1$ , use numerical integration we can have:

$$f(x) = s \sum_{n=1}^N \Phi[2\pi s(n-1 - \frac{N}{2})] e^{-i2\pi s(n-1 - \frac{N}{2})x} \tag{12}$$

$t = 2\pi s(n-1 - \frac{N}{2}), n = 1, 2, \dots, N$   
Let , bring in (12) to find the density function. The value of the four parameters from the fractal distribution can be estimated by means of the computer program. And the probability density function and the distribution function can be simulated.

The flood level at the inner seawall of the Yangtze River estuary in Shanghai consists of tidal level, storm water increase and upstream flood, which are respectively set as random variables  $X, Y, Z$ . In order to reflect their fractal characteristics, the fractal distribution function is used to describe their probability characteristics:

$$X \sim S_{\alpha_1}(\gamma_1, \beta_1, \delta_1) \tag{13}$$

$$Y \sim S_{\alpha_2}(\gamma_2, \beta_2, \delta_2) \tag{14}$$

$$Z \sim S_{\alpha_3}(\gamma_3, \beta_3, \delta_3) \tag{15}$$

The return levels of the tidal level  $X$ , the storm water increase  $Y$ , and the upstream flood  $Z$  with the return period  $N$  are  $x_p, y_p, z_p$  respectively, the relationship between the random variable distribution function and the return period  $N$  is:

$$N = \frac{1}{P(X > x)} = \frac{1}{1 - S_\alpha(x; \gamma, \beta, \delta)} \tag{16}$$

We can calculate the return levels  $x_p, y_p, z_p$  for tidal water  $X$  with the return period  $N$ , storm water increase  $Y$ , and upstream floods  $Z$  as follows:

$$x_p = S_{\alpha_1}^{-1}\left(1 - \frac{1}{N}; \gamma_1, \beta_1, \delta_1\right) \tag{17}$$

$$y_p = S_{\alpha_2}^{-1}\left(1 - \frac{1}{N}; \gamma_2, \beta_2, \delta_2\right) \tag{18}$$

$$z_p = S_{\alpha_3}^{-1}\left(1 - \frac{1}{N}; \gamma_3, \beta_3, \delta_3\right) \tag{19}$$

In hydrological statistics, the return level  $x_p$  of a random variable at the time of the return period  $N$  is defined as the event exceeding  $x_p$  every  $N$  years on

average; which also can mean that in any year, the annual maximum will exceed  $X_p$  with the probability of  $1/N$ .

**3. Calculation of Annual Return Level**

The over-threshold extremum data of Shanghai Wusong Station (1970-1989) was selected and analyzed using fractal theory. We calculated the range and the standard deviation of the data, and used the least squares method to establish the linear regression equation. The slope of  $\ln(R/S)$  to  $\ln(t)$  is the Hurst index. For the specific operation, see the following formula (20-22):

$$R(\tau) = \max_{1 \leq t \leq \tau} X(t, \tau) - \min_{1 \leq t \leq \tau} X(t, \tau) \tag{20}$$

$$S(\tau) = \sqrt{\frac{1}{\tau} \sum_{t=1}^{\tau} [X(t) - \bar{X}(\tau)]^2} \tag{21}$$

$$\ln \frac{R(\tau)}{S(\tau)} = \ln C + H \ln \tau \tag{22}$$

The Hurst index of tidal level  $X$ , storm water increase  $Y$  and upstream flood  $Z$  is calculated by R/S analysis. The calculation results are shown in table 1.

**Table 1.** Hurst index of univariate

Random Variables	X	Y	Z
Hurst index	0.5479	0.5456	0.6124

It can be seen from Table 1 that the Hurst indices of tidal water  $X$ , storm water increase  $Y$ , and upstream flood  $Z$  are  $H_x = 0.5479$ ,  $H_y = 0.5456$ ,  $H_z = 0.6124$  respectively. The Hurst index indicates that  $0.5 < H < 1$ , meaning that the tidal level, storm water increase and upstream flood have persistent state on the time scale, and appear as a trend-enhancing sequence with a long-term memory effect, that is, the previous observation will have the Long-term impact on the latter observation. The correlation scale  $C$  for measuring this effect can be calculated according to the formula  $C = 2^{2H-1} - 1$ ,  $C < 0$  indicates a negative correlation of the sequence;  $C > 0$  indicates a positive correlation of the sequence, and the results are shown in Table 2:

**Table 2.** Correlation scale  $C$  of univariate

Random Variables	X	Y	Z
Correlation scale $C$	0.0687	0.0653	0.01686

It can be seen from Table 2 that the correlation scale  $C$  of tidal water  $X$ , storm water increase  $Y$  and upstream flood  $Z$  satisfies  $C > 0$ , indicating that the over-threshold extreme time series of tidal water  $X$ , storm water increase  $Y$  and upstream flood  $Z$  are positively correlated, all shown as trend-enhanced sequences. From the correlation scale  $C_x = 0.0687$ ,  $C_y = 0.0654$ ,  $C_z = 0.01686$ , it can be seen that  $C_y < C_x < C_z$ . This means when considering the observation values of the previous period to the latter stage for those exceeding the threshold, the upstream flood has the strongest influence, the tidal water is the second, and the storm water increase has the weakest influence.

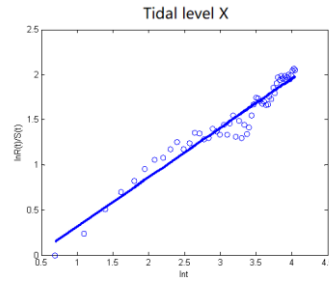


**Figure 1.** Tidal level  $\ln(R/S)$  to  $\ln(t)$

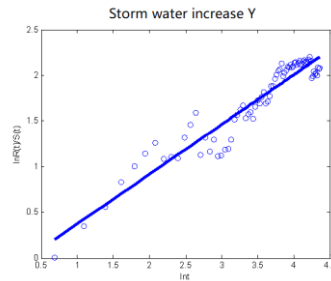


**Figure 2.** Storm water increase  $\ln(R/S)$  to  $\ln(t)$

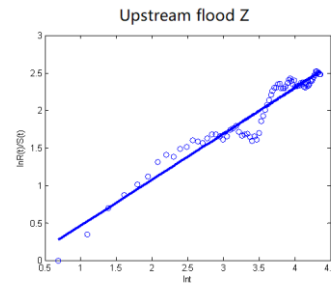


**Figure 3.** Upstream flood  $\ln(R/S)$  to  $\ln(t)$

Figure 1 - Figure 3 respectively shows the  $\ln(R/S)$  to  $\ln(t)$  relationships for the tide level, the storm water increase and the upstream flood. As can be seen from the image, there is  $R/S \sim t^H$  and the calculation results in Table 1 show that  $H_x = 0.5479$ ,  $H_y = 0.5456$ ,  $H_z = 0.6124$ . This empirical relationship can be used to correlate observations at different time scales  $t$ , providing the possibility of extrapolating large (small) scale laws from small (large) scale observations. The fractal dimension  $D$  can be calculated according to the formula  $D = 2 - H$ . The results are shown in Table 3.

**Table 3.** Univariate fractal dimension

Random Variables	X	Y	Z
Fractal Dimension $D$	1.4521	1.4544	1.3876

From the calculation results of the fractal dimension of the tidal water, storm water increase and upstream flood in Table 3  $D_x = 1.4521$ ,  $D_y = 1.4544$ ,  $D_z = 1.3876$ , it can be seen that there are obvious fractal features in the tidal level, storm water increase and upstream flood. Thus the

fractal distribution parameters for the univariate can be estimated through the program, as shown in Table 4:

**Table 4.** Fractal distribution parameters of the univariate

Random Variables	X	Y	Z
$\alpha$	1.8251	1.8865	1.6330
$\beta$	0.6586	1.0000	0.0240
$\delta$	3.6700	0.3919	0.1252
$\gamma$	0.4154	0.1886	0.0675

From the calculation results of the tidal level, storm water increase and upstream flood fractal distribution parameters in Table 4, the characteristic indices are  $\alpha_x = 1.8251$ ,  $\alpha_y = 1.8865$ ,  $\alpha_z = 1.6330$  respectively, indicating that the disaster-causing factor for the seawall overflow flooding has sharp peak and thick tail characteristics. For the skew index  $\beta$ , there are  $\beta_x = 0.6586$ ,  $\beta_y = 1.0000$ ,  $\beta_z = 0.0240$ , and there is always  $0 < \beta < 1$  indicating that the fractal distribution of the disaster causing factor is right-biased, showing the characteristics of the right thick tail, so the fractal time series for the tidal level, storm water increase and upstream flood have long-term memory effects.

The annual return level for the univariate  $N$  based on fractal distribution can be calculated by formula (17)-formula (19). The calculation results are shown in Table 5.

**Table 5.** Annual return level of univariate  $N$

Tidal level X		Storm water increase Y		Upstream flood Z	
Return period N (year)	Return level $x_p$ (m)	Return period N (year)	Return level $y_p$ (m)	Return period N (year)	Return level $z_p$ (m)
20	4.8239	20	0.9012	20	0.3126
50	5.2737	50	1.0785	50	0.4093
100	5.7479	100	1.2494	100	0.5277
200	6.4699	200	1.5010	200	0.7145

From the calculation results in Table 5, we can see that when the return period is 20 years, the return levels for the tide level, storm water increase and upstream flood are 4.8239 meters, 0.9012 meters, and 0.3126 meters respectively; when the return period is 50 years, the return levels for the tide level, storm water increase and upstream flood are 5.2737 meters, 1.0785 meters, and 0.4093 meters. When the return period is 100 years, the return levels for the tide level, storm water increase and upstream flood are 5.7479 meters, 1.2494 meters, and 0.5277 meters; when the return period is 200 years, the return levels for tidal level, storm water increase and upstream flood are 6.4699 meters, 1.5010 meters, and 0.7145 meters. It can be seen from these data that for the disaster-causing factors such as tidal level, storm water increase and upstream flood, the return level gradually increases alongside the return period extending.

**4. Conclusion**

Taking the threshold value of the Wusong station in Shanghai as a sample, and through the calculation of Hurst index, correlation dimension and fractal dimension, this study reveals that the tidal level, storm water increase and upstream flood possess obvious fractal characteristics. The conclusions can be applied to the combined risk analysis of Shanghai flood control projects and the flood risk analysis of the Yangtze River estuary in Shanghai.

This paper studies the typhoon disaster-causing factors such as storm water increase and upstream flood, which has self-similarity features on temporal and spatial scales. By the nature of fractal distribution, its parameters are derived. It can be seen from the fitting graph that the fractal distribution can better represent the sharp peak and thick tail characteristics of the variable.

Applying the fractal theory to study the time series of hydrological variables can better reveal the time scale problems and the self-similarity of hydrological phenomena. It not only can be used to better study the interactions between storm water increase and upstream flood, but it also can better present the natural characteristics of the tidal level, storm water increase and upstream flood over the time scale. It is therefore both rational and advantageous to use the fractal theory in studying the joint probability, especially for the hydrological disaster-causing factors such as the storm water increase and upstream flood. As can be seen, the fractal theories are of great value, and can also be applied to many other fields in the future where self-similarity can be found [21-22], and continue exhibiting its usefulness.

**References**

- [1] Wu Deng; Huimin Zhao; Xinhua Yang; JuxiaXiong; Meng Sun; Bo Li. Study on an improved adaptive PSO algorithm for solving multi-objective gate assignment. *Applied Soft Computing*, **2017**, 59:288-302.
- [2] B Chen; Z Yang; S Huang; X Du; Z Cui; J Bhimani; et al. Cyber-physical system enabled nearby traffic flow modelling for autonomous vehicles. 36th IEEE International Performance Computing and Communications Conference, Special Session on Cyber Physical Systems: Security, Computing, and Performance (IPCCC-CPS) IEEE. 2017.
- [3] ESCALANTE H J; PONCE-LÓPEZ V; WAN J; et al. ChaLearn Joint Contest on Multimedia Challenges Beyond Visual Analysis: An overview. 2016 23rd International Conference on Pattern Recognition (ICPR). 2016, 67-73.
- [4] B Chen; G Liu; L Wang. Predicting Joint Return Period Under Ocean Extremes Based on a Maximum Entropy Compound Distribution Model. *International Journal of Energy and Environmental Science*, **2017**, 2(6): 117-126.
- [5] PONCE-LÓPEZ V; CHEN B; OLIU M; et al. ChaLearn LAP 2016: First Round Challenge on First Impressions - Dataset and Results. *Computer Vision – ECCV 2016 Workshops*. Springer, Cham, **2016**, 400-418.
- [6] BChen; BWang. Location Selection of Logistics Center in e-Commerce Network Environments. *American Journal of Neural Networks and Applications*, Science Publishing Group, **2017**, 3(4): 40-48.
- [7] L Wang; X Xu; G Liu; B Chen; Z Chen. A new method to estimate wave height of specified return period. *Chin J OceanolLimnol*. Science Press; **2017**, 35: 1002-1009.

- [8] L-P Wang; B-Y Chen; C Chen; Z-S Chen; G-L Liu. Application of linear mean-square estimation in ocean engineering. *China Ocean Eng.* Chinese Ocean Engineering; **2016**, 30: 149-160.
- [9] G Liu; B Chen; L Wang; et al. Wave Height Statistical Characteristic Analysis. *Journal of oceanology and limnology.* **2018**, 36(4):1123-1136.
- [10] X Liu; Y He; H Fu; B Chen; M Wang; Z Wang. How Environmental Protection Motivation Influences on Residents' Recycled Water Reuse Behaviors: A Case Study in Xi'an City. *Water.* **2018**, 10, 1282.
- [11] J Song; Q Feng; X Wang; H Fu; W Jiang; B Chen. Spatial Association and Effect Evaluation of CO<sub>2</sub> Emission in the Chengdu-Chongqing Urban Agglomeration: Quantitative Evidence from Social Network Analysis. *Sustainability.* **2019**, 11, 1.1-19
- [12] L-P Wang; B Chen; J-F Zhang; Z Chen. A new model for calculating the design wave height in typhoon-affected sea areas. *Natural Hazards.* Springer Netherlands; **2013**, 67: 129-143.
- [13] S Jiang; M Lian; C Lu; S Ruan; Z Wang; B Chen. SVM-DS Fusion Based Soft Fault Detection and Diagnosis in Solar Water Heaters. *Energy Exploration & Exploitation.* **2018**, <https://doi.org/10.1177/0144598718816604>.
- [14] G Liu; B Chen; S Jiang; H Fu; L Wang; W Jiang. Double Entropy Joint Distribution Function and Its Application in Calculation of Design Wave Height. *Entropy* **2019**, 21, 64.
- [15] Baiyu Chen; Kuangyuan Zhang; Liping Wang; Song Jiang; Guilin Liu. Generalized Extreme Value - Pareto Distribution Function and Its Applications in Ocean Engineering. *Chinese Ocean Engineering.* **2019**, 2.
- [16] Baiyu Chen; Guilin Liu; Liping Wang; Kuangyuan Zhang; Shuaifang Zhang. Determination of Water Level Design for an Estuarine City. *Journal of oceanology and limnology.* **2019**.
- [17] SF Zhang; W Shen; DS Li; XW Zhang; BY Chen. Nondestructive ultrasonic testing in rod structure with a novel numerical Laplace based wavelet finite element method. *Latin American Journal of Solids and Structures.* **2018**, 15(7):1-17, e48.
- [18] G Liu; B Chen; Z Gao; H Fu; S Jiang; L Wang; K Yi. Calculation of Joint Return Period for Connected Edge Data. *Water.* **2019**, 11, 300; doi: 10.3390/w11020300.
- [19] Baiyu Chen; Tina Gui; Shiquan Cheng; Xiao Li. Research on Operation Cost in Urban Transportation System Based on Stopping Distance and Vehicle Density. *Journal of Simulation.* **2019**, 7(1):67-72.
- [20] G Liu; Z Gao; B Chen; H Fu; S Jiang; L Wang; Y Kou. Study on Threshold Selection Methods in Calculation of Ocean Environmental Design Parameters. *IEEE ACCESS.* 2019, 7, 39515-39527
- [21] Y Kou; M-C Koag; S Lee. N7 methylation alters hydrogen-bonding patterns of guanine in duplex DNA. *J Am Chem Soc.* **2015**, 137: 14067-14070.
- [22] Y Kou; M-C Koag; S Lee. Structural and Kinetic Studies of the Effect of Guanine N7 Alkylation and Metal Cofactors on DNA Replication. *Biochemistry.* **2018**, 57: 5105-5116.